



Jalalvand, M., Hosseini-Toudeshky, H., & Mohammadi, B. (2013). Homogenization of diffuse delamination in composite laminates. *Composite Structures*, 100, 113-120.
<https://doi.org/10.1016/j.compstruct.2012.12.022>

Peer reviewed version

Link to published version (if available):
[10.1016/j.compstruct.2012.12.022](https://doi.org/10.1016/j.compstruct.2012.12.022)

[Link to publication record in Explore Bristol Research](#)
PDF-document

NOTICE: this is the author's version of a work that was accepted for publication in *Composite Structures*. Changes resulting from the publishing process, such as peer review, editing, corrections, structural formatting, and other quality control mechanisms may not be reflected in this document. Changes may have been made to this work since it was submitted for publication. A definitive version was subsequently published in *Composite Structures*, [VOL 100, (2013)] DOI 10.1016/j.compstruct.2012.12.022

University of Bristol - Explore Bristol Research

General rights

This document is made available in accordance with publisher policies. Please cite only the published version using the reference above. Full terms of use are available:
<http://www.bristol.ac.uk/red/research-policy/pure/user-guides/ebr-terms/>

Homogenization of Diffuse Delamination in Composite Laminates

Meisam Jalalvand¹, Hossein Hosseini-Toudeshky^{1*}, and Bijan Mohammadi²

¹Department of Aerospace Engineering, Amirkabir University of Technology, Hafez ave.,
Tehran, Iran

²School of Mechanical Engineering, Iran University of Science & Technology, Narmak,
Tehran, Iran

Abstract

Diffuse delamination initiating from the tips of transverse cracks is usually the secondary damage mode when a composite laminate experience tensile loading. Transverse cracking has been widely investigated in analytical methods and recently, new “mechanism-based” constitutive laws were proposed for considering the cracked layer as a continuum medium. Delamination induced by matrix cracking was studied analytically, however, a proper homogenization way has not been proposed yet. In this paper, a modification to an available cohesive constitutive law is proposed to be capable of considering the effect of diffuse delamination without the necessity of consideration of an actual discontinuity between the layers. The proposed constitutive law is then compared with its equivalent models containing interlaminar discontinuity in terms of surrounding plies elasticity and distance between repetitive interlaminar cracks. It is shown that the obtained results are in good agreement with different elasticity of surrounding layers. Then the proposed modification is used in Double Cantilever Beam (DCB) specimen. Obtained results in this case are coincident with the results of an equivalent model in which diffuse discontinuity is assumed at the interface.

Introduction

When composite laminates experience tension loading, the primary damage mode is transverse cracking. The density of matrix cracks increases until a certain value known as critical or saturation crack density and beyond this value, damage may grow as diffuse delamination from the tips of transverse cracks. The interaction of transverse cracking and delamination has been widely investigated in micromechanics by analytical solutions [1-5]. In these methods, a uniform distribution of transverse cracking was assumed at each ply and therefore damage analysis could be confined in a representative volume element or unit-cell in the laminate level. Figure 1 (a) shows a typical unit-cell containing induced delamination. Both transverse and interlaminar cracks are assumed as discontinuities in the displacement field in these methods. The main drawback of the available micromechanics methods is that they are restricted in terms of layup configuration and/or loading type.

* Corresponding Author, hosseini@aut.ac.ir, Tel: +98 21 6454 3224

Another approach is the meso-scale modeling; firstly introduced to composite materials and then developed by Ladeveze, Allix and Lubineau [6-9] using continuum damage mechanics. The main concept in meso-modeling is the use of an intermediary scale related to the scale of the laminate. On this scale, two basic meso-constituents of single layer and interface, which transfer displacements and normal stresses from one ply to another one, are considered. Material models are introduced to both layer and interface using the internal variables framework and continuum damage mechanics is applied to describe their degradation. The advantage of this method is a simple damage mechanism on the constituents' scale that can be very complex on the structure's scale.

The initially proposed models for single layer damage were more inspired by classical theory of plasticity [10-11], however, it seems that the recently proposed works are more “mechanism based” [12]. In other words, the damage tensors of 2nd and 4th order in traditional formulation of CDM are exchanged to more physically based state variables such as “transverse crack density” and “diffuse delamination rate” in recent proposed methods [9, 13-15]. Figure 1 (b) shows the equivalent laminate in meso-scale modeling. The cracks or discontinuities in the traditional unit-cell are replaced by deterioration of the material properties at interfaces and damaged ply group.

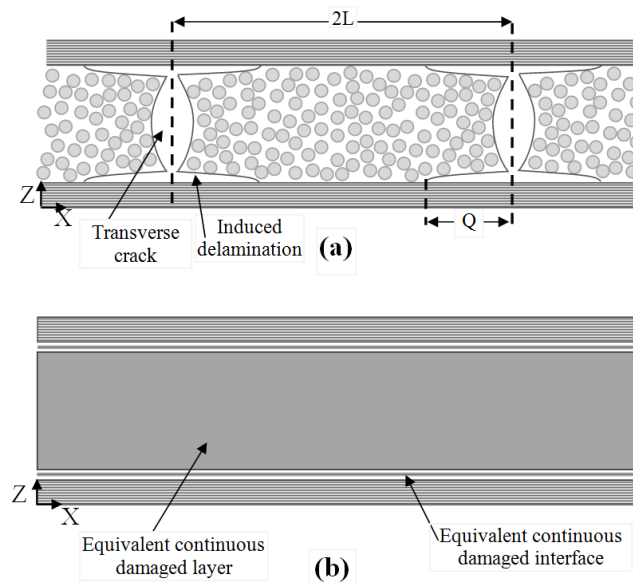


Figure 1- (a) a unit cell with evenly induced delamination from matrix cracks (b) the equivalent unit cell in meso-scale modeling

Small interlaminar cracks induced by transverse cracks have two different consequences in meso-scale modeling: (i) deteriorate the interface of the attached plies and (ii) weaken the ply group, surrounded by induced delamination, leading to generate “dead material”. The effects of induced delamination on in-plane damage variable has been recently investigated [1, 9, 15-16] and will not be addressed here. However, to the best knowledge of the authors, interface deterioration due to many interlaminar cracks has not been investigated in meso-scale modeling yet. This means that in the available meso-models, despite that the interface is weakened by

induced delamination, the employed cohesive laws have not been modified accordingly. To overcome this shortcoming, a modification to an available cohesive constitutive law is proposed in this paper considering the explained damage mode. For validation, a unit-cell with interlaminar discontinuity and another one with proposed continuous cohesive formulation are compared. The obtained results in both damage initiation and deterioration are appropriately coincident. Then to show the capability of the proposed method, crack propagation of a DCB test specimen containing diffuse delamination on its interface is compared with another model but with proposed continuous diffuse delamination. The results of both models are in agreement with each other. [I think it is not proper to enter more details here! Because it would be the same as the result and discussion part. However I included that the crack propagation of both models are compared now.]

Methodology

In this paper, effects of diffuse delamination on deterioration of the interface between two plies groups are investigated by proposing a modification to the available cohesive constitutive law. By this modification, one may use that for considering the diffuse delamination in progressive damage analysis of layered components. Transverse cracking is not considered at the first stage of developing the idea in this study as shown in Figure 2(a) and the unit-cell is assumed to comprise the interface and surrounding plies as shown in Figure 2(b). The modification of cohesive constitutive law is then proposed in the context of an equivalent unit-cell in which no real discontinuity is considered as shown in Figure 2(c). The idea behind the model is that the elastic and damage behavior of a unit-cell with a delamination of length Q under the external stresses of σ_z and σ_{xz} be the same as the equivalent unit-cell but with a new homogenized cohesive zone at the interface part. In the proposed model, the “diffuse delamination rate” with the value of Q/L is assumed to be uniform while damage grows at the interface.

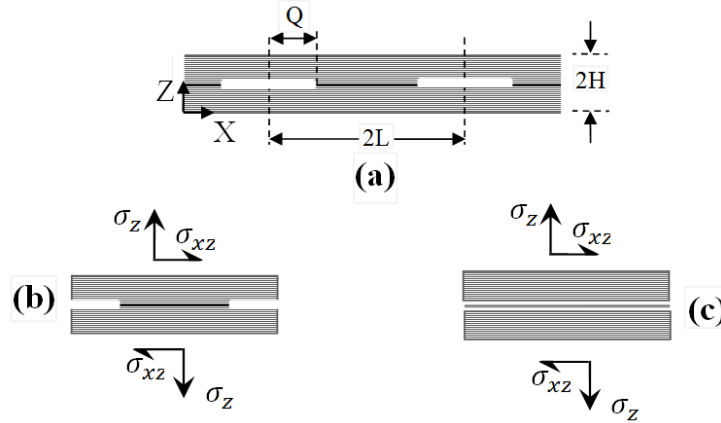


Figure 2- (a) lay-up with uniform diffuse delamination (b) unit-cell with discontinuity as delamination (c) the equivalent unit-cell with homogenized cohesive zone

The explained modification is implemented to an available bilinear cohesive constitutive law proposed in [17-18] for modeling the behavior of laminates with diffuse delamination rate of $\varphi=Q/L$. The procedure is quit straight forward and can be easily adapted for any conventional cohesive constitutive law. From cohesive side of view, φ is a nonlocal variable came up from the intralaminar damages models. Therefore, in addition to a existed damage variable as the state variable in the presented cohesive constitutive law in [17-18], the nonlocal variable of φ is introduced here as another state variable. The formulation details are presented in the following sections. In the first part of deriving the formulation, the compliance effect of the surrounding plies is not considered, but in the next step, the elasticity of the surrounding plies is taken into account.

Damage Initiation

In an ordinary cohesive constitutive law, the elastic limit stress is used to determine the initiation of damage. In the proposed homogenized unit-cell with an induced delamination rate of φ , the components of the elastic limit stresses are decreased by the ratio of $(1-\varphi)$ due to the damaged interface area. Equation (1) is the damage initiation relation of such homogenized unit-cell.

$$\sqrt{\left(\frac{\sigma_z}{(1-\varphi)T}\right)^2 + \left(\frac{\sigma_{xz}}{(1-\varphi)S}\right)^2 + \left(\frac{\sigma_{yz}}{(1-\varphi)S}\right)^2} = 1 \quad (1)$$

Where σ_i ($i=z, xz$, and yz) are stress components on the interface and T and S are tensile and shear elastic limit of stress respectively.

In the ordinary cohesive constitutive laws (without nonlocal variable of diffuse delamination), while stress is lower than the elastic limit, the damage variable of cohesive zone remains equal to zero, $D=0$. However, in the homogenized cohesive model, the stiffness of the cohesive is decreased due to the damaged area. Ignoring the compliance of the surrounding plies, the stiffness of the homogenized cohesive zone is proportional to the non-delaminated zone in the

original unit-cell by the factor of $(1 - \varphi)$. Therefore, the stress-displacement relations become as follows.

$$\sigma_i = K(1 - \varphi)\delta_i \quad (2)$$

Where δ_i ($i=z, xz$, and yz) is the relative displacement components of the cohesive zone and K is the original penalty stiffness. To find the relative elastic displacement limit, the stress components are substituted from (2) into (1). Then, the damage initiation criterion becomes as follows:

$$\sqrt{\left(\frac{\delta_z}{\delta_I^0}\right)^2 + \left(\frac{\delta_{xz}}{\delta_{II}^0}\right)^2 + \left(\frac{\delta_{yz}}{\delta_{II}^0}\right)^2} = 1 \quad (3)$$

While δ_I^0 and δ_{II}^0 are found from the following relations.

$$\begin{aligned} T &= K\delta_I^0 \\ S &= K\delta_{II}^0 \end{aligned} \quad (4)$$

Relation (3) shows that although the stress components of damage initiation in homogenized interface are reduced by diffuse delamination rate of φ , the relative displacements at damage initiation are independent from φ . Defining the mode ratio as $\beta = \delta_{II}/\delta_z$, shear displacement as

$\delta_{II} = \sqrt{\delta_{xz}^2 + \delta_{yz}^2}$ and mixed-mode displacement as $\delta_m = \sqrt{\delta_z^2 + \delta_{II}^2}$, it is possible to find the mixed-mode damage initiation displacement from (5) which has been similarly proposed in [17] too. This means that the damage initiation condition would not change by choosing the relative displacement criteria.

$$\delta_m^0 = \delta_I^0 \delta_{II}^0 \sqrt{\frac{1 + \beta^2}{\delta_{II}^{0^2} + (\beta\delta_I^0)^2}} \quad (5)$$

Figure 3 compares original bilinear cohesive law with the explained modified cohesive constitutive law considering the induced delamination with the rate of φ in mixed-mode condition. This figure shows that the damage initiation stress is decreased in the homogenized interface of the unit-cell with induced delamination, but the relative damage initiation displacements are similar for both original ($\varphi=0$) and modified cohesive law ($\varphi \neq 0$).

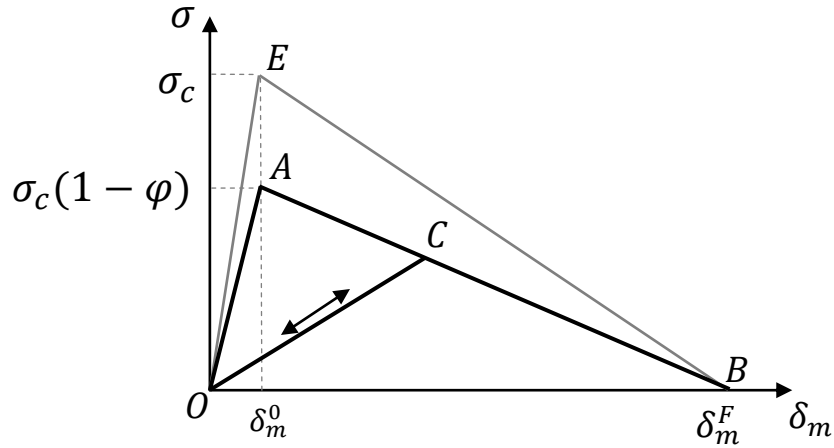


Figure 3- Comparison of original bilinear cohesive constitutive law with the one modified by diffuse delamination rate of ϕ

Damage propagation

Various criterions have been proposed in mixed-mode crack propagation of cohesive constitutive modeling. The proposing nonlocal constitutive law can be used with many of them and the mixed-mode criterion proposed by the Benzeggagh and Kenane [19] is used here. For homogenized cohesive constitutive law, since the un-cracked area of the unit-cell is reduced by the ratio of $(1 - \phi)$, it is assumed that the critical energy release rate of the cohesive zone associated with the studied unit-cell in meso-scale modeling is reduced by the same ratio. This can be interpreted as equivalency of energy absorption capacity of both original and continuous interfaces. For a mixed-mode case of I and II loading condition in a homogenized interface with diffuse delamination rate of ϕ , this criterion is defined as follows.

$$(1 - \phi)G_{IC} + (1 - \phi)(G_{IIC} - G_{IC}) \left(\frac{G_{II}}{G_I + G_{II}} \right)^\eta = (1 - \phi)G_C \quad (6)$$

Where, G_{IC} , G_{IIC} and G_C are mode I, mode II and mixed-mode critical energy release rate. G_I and G_{II} are also the energy release rates at a certain gauss point. η is also a material constant which can be determined by tests under different mode ratios. The term $(1 - \phi)$ reflects the decrease in capacity of energy absorption of the homogenized interface here and it vanishes when there is no diffuse delamination. The value of $G_{II}/(G_I + G_{II})$ depends on the mixed-mode ratio of ' β '.

Obviously, the term $(1 - \phi)$ can be easily omitted from both side of (6) and then the criterion is not changed comparing with the original one without the effect of defuse delamination. Since this criterion is used for calculation of critical relative displacement in mixed-mode, δ_m^F , it means that although diffuse delamination decrease the capability of energy absorption, the δ_m^F doesn't depend on the diffuse delamination rate. This point is taken into account in Figure 3 as well. Therefore, the critical relative displacement is as follows. More details can be found in [17].

$$\delta_m^F = \frac{2}{K\delta_m^0} \left(G_{IC} + (G_{IIC} - G_{IC}) \left(\frac{\beta^2}{1 + \beta^2} \right)^\eta \right) \quad \text{if } \delta_l > 0 \quad (7)$$

Constitutive law

While cohesive element is not under pressure ($\delta_l \geq 0$), the relationship between stress and relative displacement becomes as follows.

$$\begin{cases} \sigma_i = K(1 - \varphi)\delta_i & \text{if } \delta_m \leq \delta_m^0 \\ \sigma_i = K(1 - D)\delta_i & \text{if } \delta_m^F > \delta_m > \delta_m^0 \\ \sigma_i = 0 & \text{if } \delta_m \geq \delta_m^F \end{cases} \quad (8)$$

The difference between the first and second conditions in Equation (8) is that φ remains constant in cohesive constitutive law, therefore when $\delta_m \leq \delta_m^0$, σ_i is calculated straightly in an elastic way. But, when $\delta_m^F > \delta_m > \delta_m^0$, the damage variable of D is firstly calculated in cohesive constitutive law, and then the stresses are found from Equation (8) which means that the solution procedure would be iterative. It is worth to note that the damage parameter “ D ” depends on the factor of $(1 - \varphi)$ as will be shown later in this section. In crack closure ($\delta_z < 0$), the normal stress is calculated without considering any damage variable from $\sigma_z = K\delta_z$ and it also doesn't take part in the damage growth.

The damage variable D can now be calculated by relating the slope of an arbitrary point with $\delta_m^F > \delta_m > \delta_m^0$ like OC to line OA in Figure 3. After some manipulation, D of a homogenized cohesive zone can be found as follows:

$$D = 1 - (1 - \varphi) \frac{(\delta_m^F - \delta_m^{max})\delta_m^0}{(\delta_m^F - \delta_m^0)\delta_m^{max}} \quad (9)$$

Where δ_m^{max} is the maximum relative displacement occurred in the cohesive zone and in monotonic loading it is equal to δ_m .

Effect of surrounding layers

In the assumed unit-cell (Figure 2 (b) and (c)), the capacity of energy absorption is just related to the cohesive zone, however the stiffness of the whole unit-cell is affected by both stiffness of cohesive zone and adjacent ply groups. If the stiffness of the layers is not much larger than the stiffness of the interface (which is usually the case), it is necessary to take into account the stiffness of the surrounding layer. In 2D model shown in Figure 2 (b), if a uniform infinitesimal displacement in z -direction, δ_z , is applied to the top surface of the unit-cell, the stress in z -direction is fairly 0 in the detached part of the laminate and σ_z in other parts. The ratio of applied force, F_z , to the applied displacement, δ_z , is assumed to be the stiffness of the unit-cell in z -direction as follows:

$$S_z = \frac{F_z}{\delta_z} = \frac{2(L - Q)}{\frac{2H}{E_z} + \frac{1}{K}} \quad (10)$$

The stiffness of the equivalent unit-cell shown in Figure 2(c) can be found similarly as follows:

$$\dot{S}_z = \frac{\dot{F}_z}{\dot{\delta}_z} = \frac{2L}{\frac{2H}{E_z} + \frac{1}{\dot{K}_z}} \quad (11)$$

[all of the equations are re-written in another editor, and they will be corrected there- regarding your comment on prime in the equations]

Where, the prime sign shows the values in equivalent unit-cell. The subscript z is added to \dot{K} to show that this value is just for the stiffness of the laminate in mode-I. Because shear stiffness is different from normal stiffness of the ply, the equivalent stiffness of the cohesive constitutive law is affected differently for various loading directions. To achieve the coincident behavior of both unit-cells in elastic condition, it is necessary that $S_z = \dot{S}_z$. Then the value of penalty stiffness in the equivalent cohesive zone can be determined from the following relation.

$$\dot{K}_z = \frac{1 - \varphi}{\frac{1}{K} + \varphi \frac{2H}{E_z}} \quad (12)$$

Apparently when the neighboring layers of the interface is very thin or very stiff, the term “ H/E_z ” in the denominator of Equation (12) is almost zero. Similarly, the shear stiffness of the cohesive zone can be calculated as follows.

$$\dot{K}_{xz} = \frac{1 - \varphi}{\frac{1}{K} + \varphi \frac{2H}{G_{xz}}} \quad (13)$$

Where G_{xz} is the shear modulus of the plies around the cohesive zone.

Numerical results

In this part, firstly the stress-displacement response of a unit-cell with modified cohesive constitutive law is compared with the response of a unit-cell with real delamination as discontinuity in the geometry. Then real conventional specimens are modeled with the proposed cohesive constitutive law.

Unit-cell with rigid plies

External normal stress in the z-direction is applied to the top surface of a unit-cell with 0° layers around the interface with the material properties listed in Table 1. The bottom of the interface is assumed to be fixed in the z-direction at all nodes and top surface nodes are uniformly displaced in the z-direction. The value of E_3 is spuriously increased to make a rigid ply condition around

the interface. Therefore, it is expected that the response of the whole laminate in the z-direction would be almost the pure response of the cohesive zone.

Table 1. Unit-cell properties for rigid ply example

Mechanical properties of the ply				Interface properties					Unit-cell	
E_1 (GPa)	E_3 (GPa)	ν_{31}	G_{12} (GPa)	G_{IC} (N/mm)	G_{IIC} (N/mm)	K (N/mm ³)	T (MPa)	S (MPa)	L (mm)	H (mm)
138e3	8.9e5	0.3	7e3	0.222	0.99	1.0e5	51.7	91.7	3	0.25

The obtained FEM results for using the explained approaches and considering of two diffuse delamination ratios of $\varphi = 1/3$ and $\varphi = 2/3$ are depicted in Figure 4. Obviously, the behavior of the unit-cell with real discontinuity is well approximated by the proposed homogenized model. The value of initial elastic stiffness of the cohesive zone was also calculated using both Equations (12) and (2) and shown in

Table 2. Because of the assumed large value of E_3 , the obtained results from two equations are very close to each other.

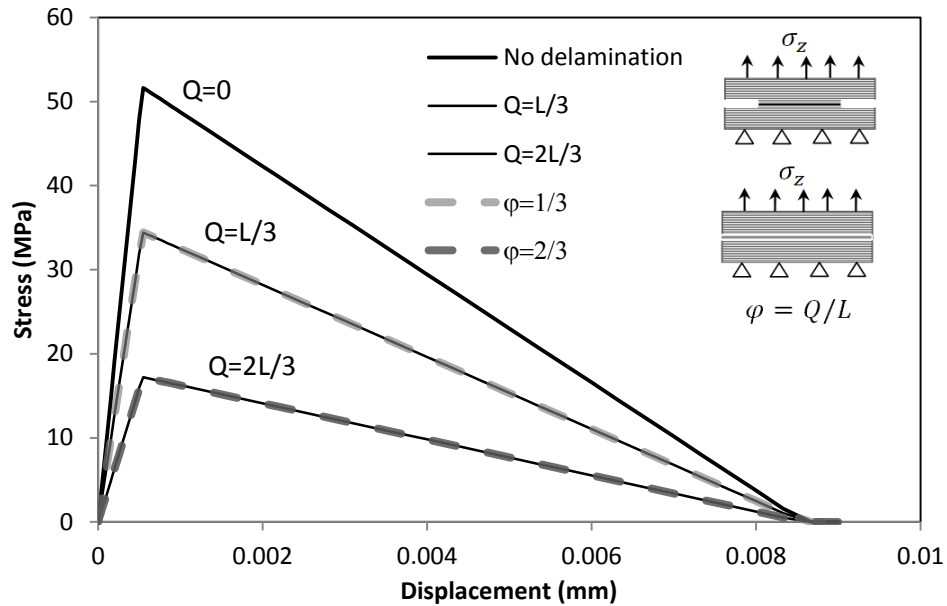


Figure 4- Applied stress vs. displacement for unit-cell with rigid plies considering diffuse delamination and the proposed cohesive constitutive law

Table 2. Elastic stiffness of the cohesive zone for unit-cell with rigid layers obtained from (12) and (2)

φ	\dot{K} from Equation (2) N/mm ³	\dot{K} from Equation (12) N/mm ³
1/3	0.666e5	0.654e5
2/3	0.333e5	0.321e5

Unit-cell with elastic plies

The previous problem is resolved while the material modulus in the z-direction is changed back to a real carbon/epoxy material property of $E_3=8.9e3$ N/mm², $\nu_{13}=0.3$ and all other values in Table 1 are reused. The numerical simulation is repeated by the same boundary conditions on top and bottom of the unit-cell and the obtained results for original unit-cell (with diffuse delamination) and one with the proposed cohesive constitutive law is depicted in Figure 5. Obviously the value of critical relative displacement δ_m^F and elastic stress limit in all of the cases are coincident which shows that the absorbed energy in each case is similar to its equivalent unit-cell. The initial stiffness of the equivalent unit-cell is also in agreement with the original unit-cell result for both considered delamination ratios. To show the effect of the Equation (12), the stress-displacement behavior of the unit-cell using Equation (2) is also depicted for the case $\varphi = 1/3$. The critical relative displacement and elastic limit are acceptable but the initial stiffness of the unit-cell is more close to the unit-cell with no delamination, $Q=0$. This is due to ignoring the term “ H/E_z ” in the denominator of Equation (12). Table 3 also shows the considerable difference between the values of initial stiffness obtained from Equations (2) and (12).

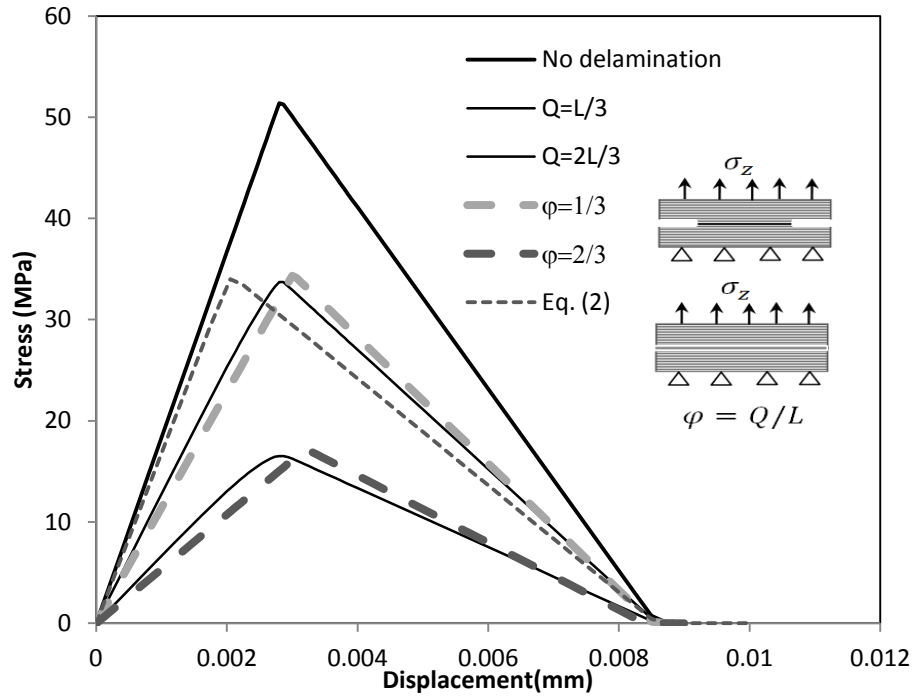


Figure 5- Applied stress vs. displacement for unit-cell with elastic plies considering diffuse delamination and the proposed cohesive constitutive law

Table 3. Elastic stiffness of the cohesive zone for unit-cell with elastic layers obtained from (12) and (2)

φ	\dot{K} from Equation (2) N/mm ³	\dot{K} from Equation (12) N/mm ³
1/3	0.666e5	0.234e5
2/3	0.333e5	7061.8

DCB Specimen

To show the capability of the proposed method, crack propagation of a DCB specimen is modeled by the explained two approaches. The selected DCB specimen is already analyzed using cohesive elements in [20]. The material properties are similar to those used in the last section for the analysis of unit-cell with elastic plies and diffuse delamination. The length, width and thickness of the specimen are 150 mm, 25.4 mm and 3.05 mm respectively and the length of pre-cracked part is also 31.75 mm as shown in Figure 6 along with the mesh scheme. The applied load versus opening displacement of the end point are compared with the results of [20] in Figure 7 and seems valid. Then the same specimen with a periodic interlaminar crack size of 0.1 mm and a distance of 0.4 mm on the interface is also assumed to investigate the effects of diffuse delamination on main interlaminar crack. This means that between each 0.4 mm of regular cohesive elements, a discontinuity of 0.1 mm was embedded at the interface. Such a diffuse

delamination scheme means that the diffuse delamination rate, φ , is equal to 0.2 and the length of the unit-cell is 0.5 mm. The problem was also analyzed without considering any real discontinuity at the interface, but using the modified cohesive constitutive law assuming $\varphi = 0.2$. The obtained results from both techniques are also presented in Figure 7. Obviously, the obtained results are coincident which means that the proposed modification for diffuse delamination could model the behavior of the diffuse delamination without a need to considering any real discontinuity in the model.

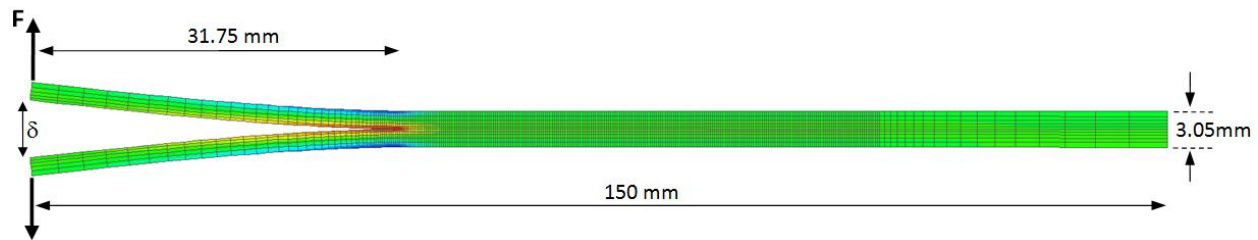


Figure 6- DCB specimen and applied mesh scheme

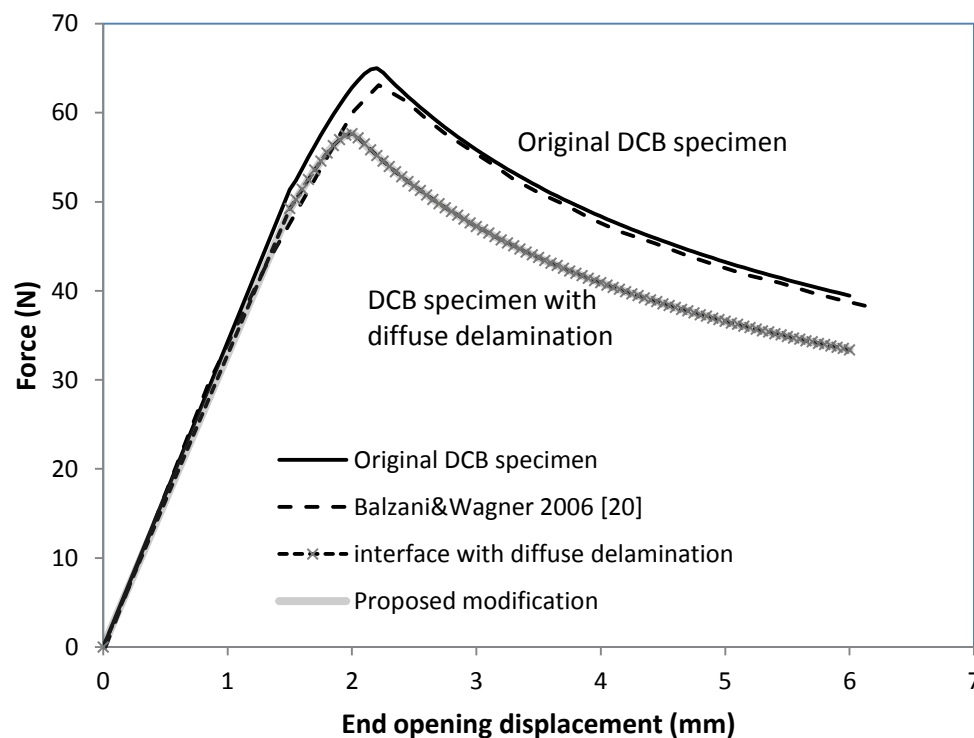


Figure 7- numerical results of the DCB for original and “diffuse-delaminated” specimen

Unit-cell length may affect the results of such analyses. Figure 8 shows the obtained results for the same diffuse delamination rate ($\varphi = 0.2$) but different unit-cell lengths of 0.5 mm, 1.0 mm, 2.0 mm and 4.0 mm using real discontinuity as the interlaminar crack at the interface. It shows that the obtained results for various unit-cell lengths other than 4.0 mm are in agreement with

those obtained from the proposed modification for considering diffuse delamination. However, for the unit-cell length of 4.0 mm, the original response includes more details and the proposed cohesive constitutive law could just capture the average response of that. The reason of behavior can be interpreted by the process zone length. Figure 9 indicates the normal stress distribution in the z-direction exactly at the crack tip in the mentioned models with various unit-cell lengths. The process zone length in all cases is almost equal, however, for unit-cell lengths of 0.5 mm, 1.0 mm, 2.0 mm the process zone is spread over three or more unit-cells, however, for the unit-cell length of 4.0 mm, the process zone is located mainly in only one unit-cell. Therefore, the response of this specimen with unit-cell length of 4.0 mm, becomes oscillatory and homogenization of such a behavior obviously loses some details, though it could properly capture the average.

[Unfortunately I am not aware of thickness of the one ply in the main reference. (it is not mentioned in the main reference)]

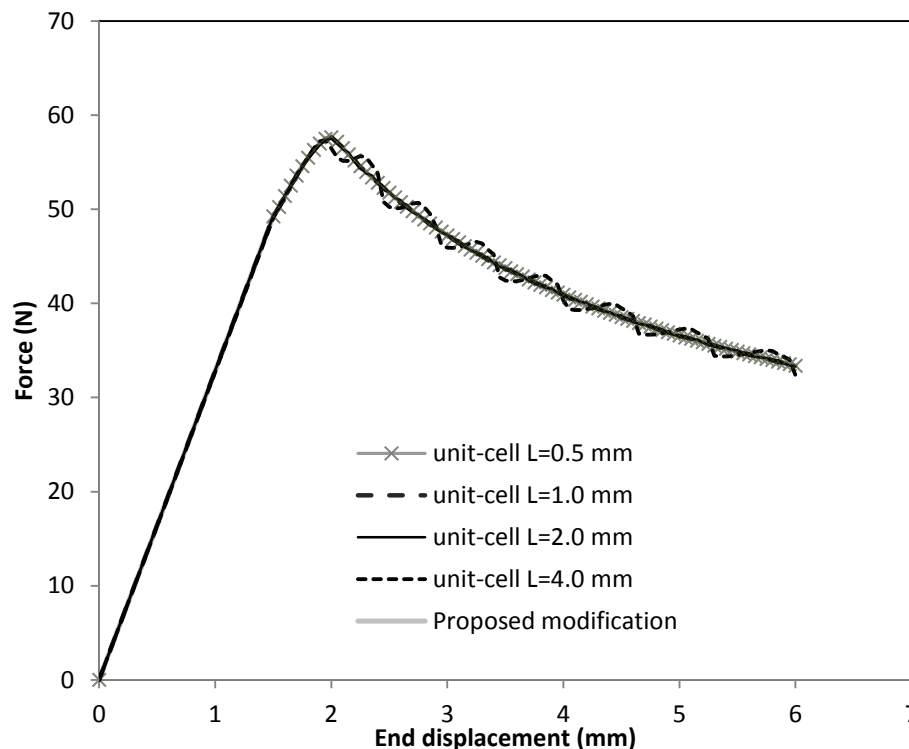


Figure 8- numerical results of the DCB specimen with diffuse delamination

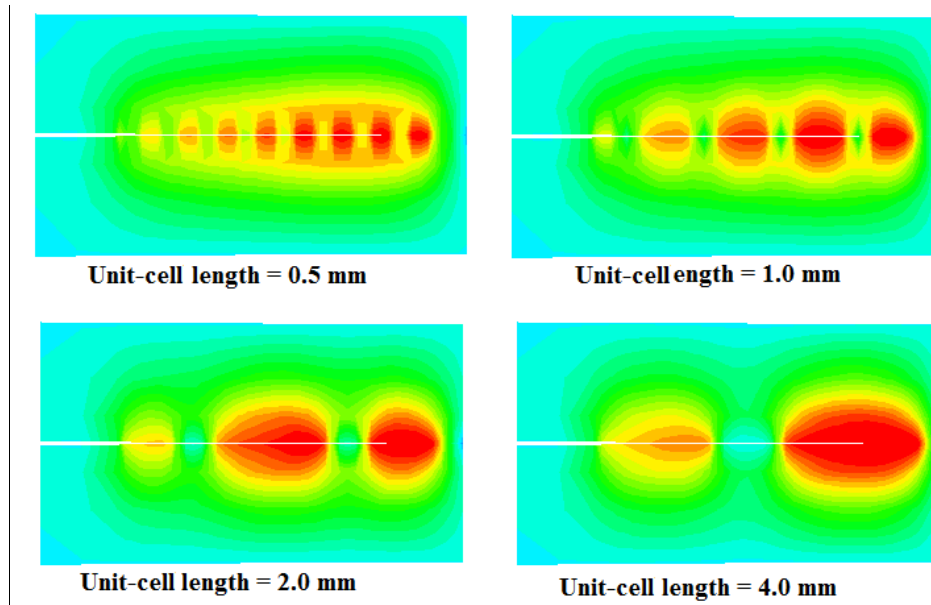


Figure 9- process zone at the crack-tip of DCB specimen

Cross-ply laminate under out-of-plane loading

The effect of the mentioned modification on the cohesive constitutive law can be shown by the lateral stiffness of the whole laminate. A cross-ply laminate of $[0/90_4]_s$ with the material properties listed in Table 1 and ply thickness of 0.125 mm is assumed. The length of the specimen is 12 mm with a unit width. The laminate is assumed to contain the uniform transverse crack spacing of $L=2$ mm and diffuse delamination rate of $\varphi=1/2$. The analyses in this part comprises the solution of four different conditions: i) laminate without any damage, ii) laminate with discontinuities as transverse and interlaminar cracks, iii) laminate with homogenized damaged 90° layers and ordinary cohesive constitutive law, and iv) laminate with homogenized damaged 90° layers along with the new proposed modification of cohesive law in section 2.

In the first step, the laminate is assumed under a uniform tensile loading to find the homogenization properties. The damage variable of 90° layers group (φ_{90°), which represents the deterioration of these layers, is related to the longitudinal stiffness of the whole laminate ($E_{x\text{ LAM}}$) using (14). This means that in the homogenization of such a damaged laminate, the stiffness of the 90° layers is equal to $(1 - \varphi_{90^\circ})E_2$. Determination of in-plane damage variables such as φ_{90° is in fact the responsibility of the applied continuum damage models. However, those modeling and procedures are not employed here and the damage variable is directly derived by the equality of stiffness of the two models with discontinuous and homogenized damage. So, the obtained damage variable is expected to be more accurate and consistent with the original model.

$$E_{x\text{ LAM}} = \frac{E_1 t_{0^\circ} + (1 - \varphi_{90^\circ}) E_2 t_{90^\circ}}{t_{90^\circ} + t_{0^\circ}} \quad (14)$$

The obtained tensile stress values for the 1% applied tensile strain of the mentioned four cases are mentioned in Table 4. By finding the laminate stiffness value of the cracked model, it is possible to calculate the damage variable of 90° (φ_{90°) layers and their effective elastic modulus from (14). For the mentioned damage scheme on the laminate, the damage variable can be calculated, $\varphi_{90^\circ}=82.31\%$, which means that the 90° layers are significantly damaged. Using such a damage variable for homogenizing of the 90° layers $E_x = (1 - \varphi_{90^\circ})E_2$, it is possible to check the obtained stress for 1% applied strain as mentioned in Table 4. This value for both cases of the modified and un-modified cohesive laws is similar and it is slightly different from the model with discontinuous cracks by about 0.6%.

Table 4. Tensile stress and lateral load for different models of $[0/90_4]_s$ cross-ply laminate

no.	model condition	tensile stress (Mpa) at $\varepsilon=1\%$	3-point Bending Force (N)
1	no damage	349.75	233.29
2	crack as discontinuity with contact elements	288.68	149.44
3	homogenized damaged 90° layers with usual cohesive law	290.38	200.38
4	homogenized damaged 90° layers with modified cohesive law	290.38	155.04

In the second step, the laminate is assumed under the 3-point bending load with span of 12 mm and applied displacement of 1 mm at the middle (Figure 10). For the assumed laminate, $L=2$ mm, $Q=1$ mm, the diffuse delamination rate becomes, $\varphi=0.5$. The shear penalty stiffness of the cohesive elements at the interface of $0^\circ/90^\circ$ layers according to (13) becomes $K_{xz}'=3439$ N/mm³. The normal value of the penalty stiffness of the cohesive elements is assumed to remain unchanged because of the compressive normal stress between $0^\circ/90^\circ$ interface.

The obtained concentrated load for each case is listed in Table 4. The lateral force of the cracked laminate, which is the representative of the lateral stiffness of the laminate, is about 36% lower than the laminate with no damage. A proper homogenized model should be able to correctly simulate both axial and longitudinal stiffness. The obtained out-of-plane load of the laminate with homogenized damaged 90° layers in the case of usual cohesive law is considerably different from the case with the modified cohesive law as listed in Table 4. The difference of cracked and homogenized model with usual cohesive elements is 34.1% but this value decreases to 3.7% when comparing the results of the homogenized model with modified cohesive law. It can be concluded that despite the model with unmodified cohesive constitutive law predicted the axial stiffness decrease properly, but it is not enough accurate for the prediction of lateral stiffness decrease. On the other hand, the combination of continuous damage model for 90° layers and the proposed modification for cohesive constitutive law (Figure 10 (b)) which is much simpler than the cracked laminate (Figure 10 (a)) is accurate enough for prediction of both axial and lateral stiffness.

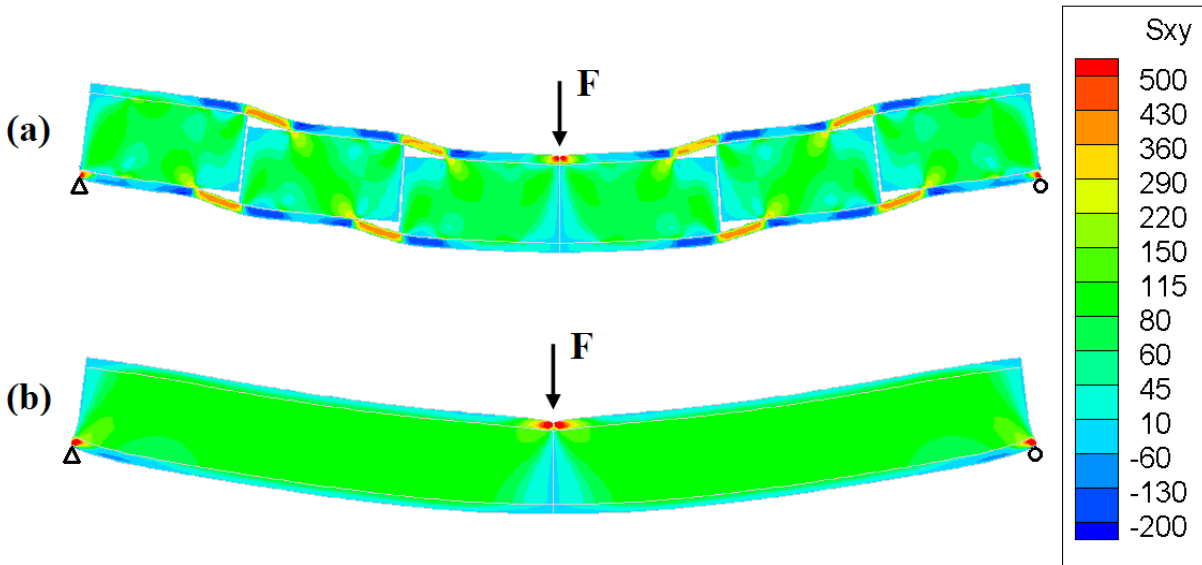


Figure 10 (a) the cracked laminate (b) the homogenized damaged laminate under 3-point bending

Conclusion

In this paper, a new simple nonlocal modification for an available cohesive constitutive law for homogenization of diffuse delamination was proposed. The predicted results using this new approach were compared with the models of a unit-cell and a DCB specimen in which diffuse delamination are implemented as discontinuities on the interface and they were found in good agreement with each other. While unit-cell length is shorter than the process zone, the predicted results of the model is coincident with the obtained results from the original models, in which diffuse delamination are treated as discontinuities. In the case of longer distance between the interlaminar cracks, if the load-displacement curve behaves oscillatory, the proposed model can properly predict the average of such a curve. Finally, it was shown that using the usual unmodified cohesive constitutive law would lead to inaccurate prediction of lateral stiffness of a laminate with transverse crack and delamination, however by using the proposed cohesive constitutive law the obtained out-of-plane force was acceptable.

1. Farrokhabadi, A., H. Hosseini-Toudeshky, and B. Mohammadi, *A generalized micromechanical approach for the analysis of transverse crack and induced delamination in composite laminates*. Composite Structures, 2011. **93**(2): p. 443-455.
2. Hashin, Z., *Analysis of cracked laminates: a variational approach*. Mechanics of Materials, 1985. **4**(2): p. 121-136.
3. McCartney, L.N., *PREDICTING TRANSVERSE CRACK FORMATION IN CROSS-PLY LAMINATES*. Composites Science and Technology, 1998. **58**(7): p. 1069-1081.
4. Nairn, J.A. and S. Hu, *The Initiation and Growth of Delamination Induced by Matrix Microcracks in laminated Composites*. International Journal of Fracture, 1992. **57**: p. 1-24.
5. Takeda, N. and S. Ogihara, *Initiation and growth of delamination from the tips of transverse cracks in CFRP cross-ply laminates*. Composites Science and Technology, 1994. **52**(3): p. 309-318.
6. Allix, O. and P. Ladevèze, *Interlaminar interface modelling for the prediction of delamination*. Composite Structures, 1992. **22**(4): p. 235-242.
7. Ladeveze, P., *A damage mechanics for composites materials*, in *Integration of theory and applications in applied mechanics*, J.F. Dijkstra and F.T.M. Nieuwstadt, Editors. 1990, Kluwer Academic Publishers: Dordrecht.
8. Ladevèze, P., *A damage computational method for composite structures*. Computers & Structures, 1992. **44**(1-2): p. 79-87.
9. Ladevèze, P., G. Lubineau, and D. Marsal, *Towards a bridge between the micro- and mesomechanics of delamination for laminated composites*. Composites Science and Technology, 2006. **66**(6): p. 698-712.
10. Barbero, E.J. and L. De Vivo, *A Constitutive Model for Elastic Damage in Fiber-Reinforced PMC Laminae*. International Journal of DAMAGE MECHANICS, 2001. **10**: p. 73-93.
11. Ladeveze, P. and E. LeDantec, *Damage modelling of the elementary ply for laminated composites*. Composites Science and Technology, 1992. **43**(3): p. 257-267.
12. Allix, O. and F. Hild, *Continuum Damage Mechanics of Materials and structures: Present and Future*, in *Continuum Damage Mechanics of Materials and structures*, O. Allix and F. Hild, Editors. 2002, Elsevier.
13. Barbero, E.J. and D.H. Cortes, *A mechanistic model for transverse damage initiation, evolution, and stiffness reduction in laminated composites*. Composites Part B: Engineering, 2010. **41**(2): p. 124-132.
14. Li, S., S.R. Reid, and P.D. Soden, *A continuum damage model for transverse matrix cracking in laminated fibre-reinforced composites*. Philosophical Transactions of the Royal Society of London, Series A, 1998. **356**(1746): p. 2379-2412.
15. Farrokhabadi, A., H. Hosseini-Toudeshky, and B. Mohammadi, *Damage analysis of laminated composites using a new coupled micro-meso approach*. Fatigue & Fracture of Engineering Materials & Structures, 2010. **33**(7): p. 420-435.
16. Abisset, E., F. Daghia, and P. Ladevèze, *On the validation of a damage mesomodel for laminated composites by means of open-hole tensile tests on quasi-isotropic laminates*. Composites Part A: Applied Science and Manufacturing, 2011. **42**(10): p. 1515-1524.
17. Camanho, P.P., C.G. Davila, and M.F. de Moura, *Numerical Simulation of Mixed-Mode Progressive Delamination in Composite Materials*. Journal of Composite Materials, 2003. **37**(16): p. 1415-1438.
18. Davila, C.G., P.P. Camanho, and M.F. de Moura, *Mixed-Mode Decohesion Elements for Analyses of Progressive Delamination*, in *42nd AIAA/ASME/ASCEIAHS/ASC Structures, Structural Dynamics and Materials Conference*. 2001: Seattle, Washington. p. Paper AIAA-01-1486.

19. Benzeggagh, M.L. and M. Kenane, *Measurement of mixed-mode delamination fracture toughness of unidirectional glass/epoxy composites with mixed-mode bending apparatus*. Composites Science and Technology, 1996. **56**(4): p. 439-449.
20. Balzani, C. and W. Wagner, *An interface element for the simulation of delamination in unidirectional fiber-reinforced composite laminates*. Engineering Fracture Mechanics, 2008. **75**(9): p. 2597-2615.